*Article*

# Controls on Soft Tissue and Cellular Preservation in Late Eocene and Oligocene Vertebrate Fossils from the White River and Arikaree Groups of Nebraska, South Dakota, and Wyoming

John E. Gallucci [1,2] , Grace Woolslayer [1], Kelsey Barker [3], Brian Kibelstis [1], Allison R. Tumarkin-Deratzian [1], Paul V. Ullmann [4], David E. Grandstaff [1] and Dennis O. Terry, Jr. [1,*]

1   Department of Earth & Environmental Science, Temple University, Philadelphia, PA 19122, USA;
    john.gallucci@mines.sdsmt.edu (J.E.G.); grand@temple.edu (D.E.G.)
2   South Dakota School of Mines and Technology, Rapid City, SD 57701, USA
3   Department of Geology, Rowan University, Glassboro, NJ 08028, USA
4   Harold Hamm School of Geology & Geological Engineering, University of North Dakota,
    Grand Forks, ND 58202, USA
*   Correspondence: doterry@temple.edu

**Abstract:** Previous studies on microtaphonomy have identified multiple types of organic microstructures in fossil vertebrates from a variety of time periods and past environmental settings. This study investigates potential taphonomic, paleoenvironmental, and paleoclimatic controls on soft tissue and cellular preservation in fossil bone. To this end, fifteen vertebrate fossils were studied: eight fossils collected from the Oligocene Sharps Formation of the Arikaree Group in Badlands National Park, South Dakota, and seven fossils from formations in the underlying White River Group, including the Oligocene Brule Formation of Badlands National Park, and the Eocene Chadron Formation of Flagstaff Rim, Wyoming; Toadstool Geologic Park, Nebraska; and Badlands National Park, South Dakota. A portion of each fossil was demineralized to identify any organic microstructures preserved within the fossils. We investigated several factors which may have influenced cellular/soft tissue decay and/or preservation pathways, including taxonomic identity, paleoclimatic conditions, depositional environment, and general diagenetic history (as interpreted through thin section analysis). Soft tissue microstructures were preserved in all fossil samples, and cellular structures morphologically consistent with osteocytes were recovered from 11 of the 15 fossil specimens. Preservation of these microstructures was found to be independent of taxonomy, paleoclimate regime, apatite crystallinity, depositional environment, and general diagenetic history, indicating that biogeochemical reactions operating within microenvironments within skeletal tissues, such as within individual osteocyte lacunae or Haversian canals, may exert stronger controls on soft tissue and biomolecular decay or stabilization than external environmental (or climatic) conditions.

**Keywords:** fossil bones; geologic age; depositional environment; paleoclimatic conditions

## 1. Introduction

The dramatic global climate change that occurred at the Eocene–Oligocene boundary has been the focus of extensive paleontological and paleoenvironmental study (e.g., [1–4]). During the Eocene-Oligocene transition (approximately 34–33 million years ago), global temperatures cooled and terrestrial landscapes became drier, with the vast forests that covered much of the world in the Paleocene and Eocene giving way to grasslands and shrub prairies [3]. This shift in climate and environments led to accompanying shifts in terrestrial faunas, especially in North America [2]. The terrestrial Eocene–Oligocene transition is preserved in the strata of the White River Group, which spans multiple states across the Great Plains and records several million years, from the late Eocene to the Middle Oligocene (Figure 1). Badlands National Park in southwestern South Dakota contains a

well-preserved section of the White River Group, with both Eocene and Oligocene strata present and easily accessible within the park boundaries. Previous work on the Badlands has detailed the paleoecology, stratigraphy, and paleopedology of these strata, including the White River Group and the lower Arikaree Group (summarized in [4]). However, the uppermost White River Group (Poleslide Member) and the lowermost Arikaree Group (Sharps Formation) in Badlands National Park have yet to be rigorously studied from lithostratigraphic and paleopedological perspectives (Figures 2 and 3).
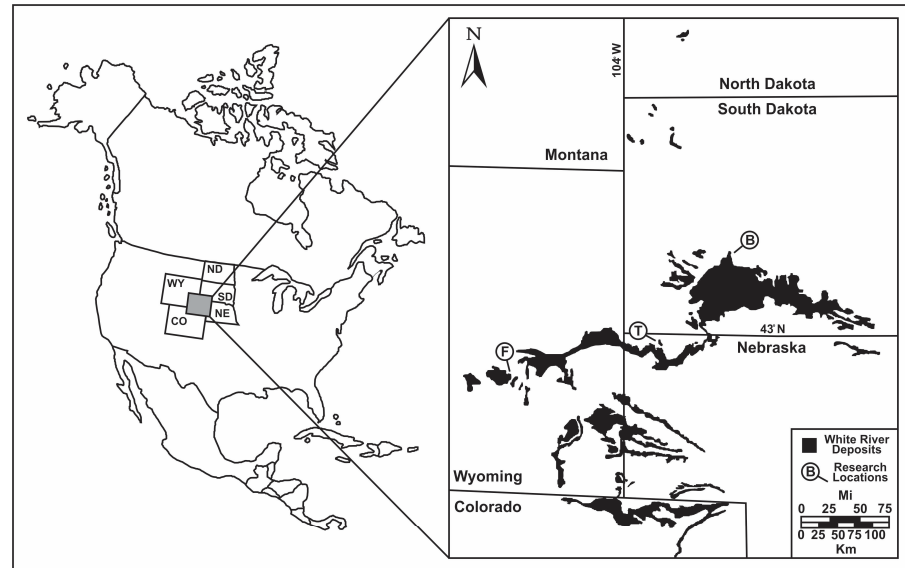


**Figure 1.** Map of White River Group deposits across the western United States. Source localities of the fossils used in this study are marked with letters. F: Flagstaff Rim, WY. T: Toadstool Geologic Park, NE. B: Badlands National Park, SD. Modified from [1].



**Figure 2.** White River and Arikaree Group strata in Badlands National Park, SD, USA. CPF: Chamberlain Pass Formation (late Eocene); PPM: Peanut Peak Member of the Chadron Formation (late Eocene); SM: Scenic Member of the Brule Formation (early Oligocene); PM: Poleslide Member of the Brule Formation (Oligocene); RFA: Rockyford Ash; SF: Sharps Formation (Oligocene). Black lines represent approximate boundaries between units. The RFA, as currently defined, represents the basal unit of the Arikaree Group in this region. Photo by D. Terry.
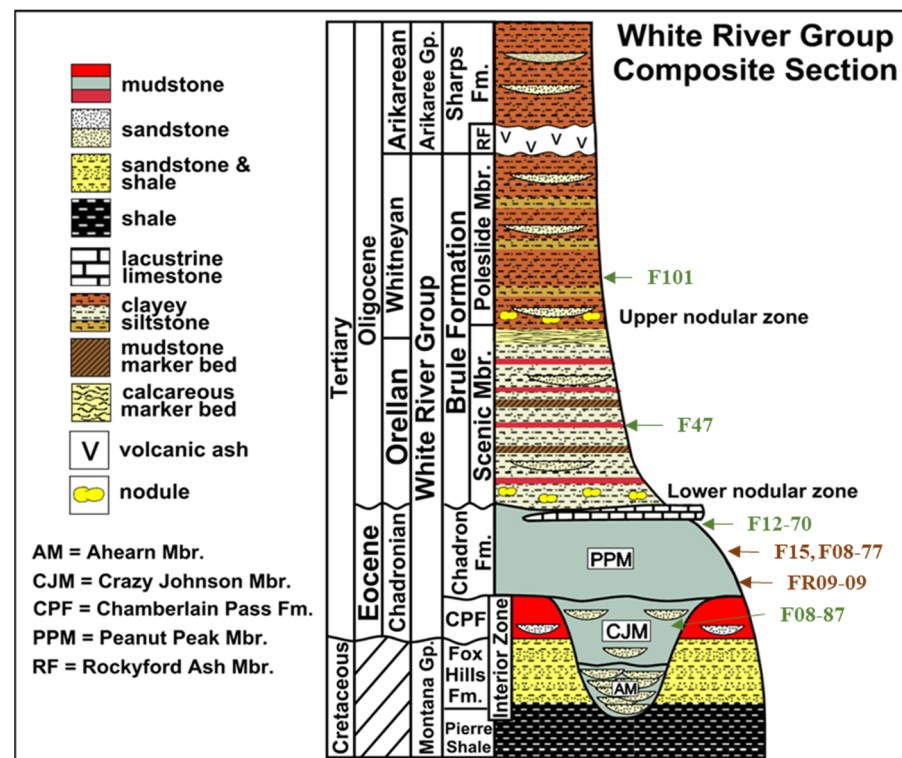
**Figure 3.** Composite section of the White River Group (not to scale) in Badlands National Park, SD, USA. Relative stratigraphic locations of the White River fossils used in this study are marked with green and brown sample numbers and arrows. Green = tortoise, brown = mammal. Note that the Rockyford Ash is equivalent to the "Cedar Pass white layer" [4]. Modified from [5].

Multiple studies have identified soft tissue and cellular structures within vertebrate fossils that are morphologically consistent with those present in extant vertebrates (e.g., [6–12]). Further studies using immunoassays and Liquid Chromatography–Tandem Mass Spectrometry (LC-MS/MS) have found that soft tissue microstructures preserved in fossils often contain remnants of endogenous biomolecules (e.g., [13,14]). However, most prior studies have focused on Mesozoic or older vertebrate fossils (e.g., [6,7]) with few exceptions (e.g., [9,15,16]), while Cenozoic vertebrates remain relatively unexplored in terms of cellular and soft tissue preservation.

The environmental, taphonomic, and sedimentologic conditions which facilitate such remarkable preservation in fossil bone remain poorly characterized. Therefore, our goal was to evaluate paleoenvironmental influences on soft tissue preservation by conducting an integrative investigation into the lithology, vertebrate taphonomy, and paleoenvironmental conditions of the Oligocene Sharps Formation, which in turn would allow us to discern the potential controls on soft tissue and cellular preservation within vertebrate fossils from the White River Group and lower Arikaree Group. Results from Oligocene fossils collected in Badlands National Park are compared to those from older Oligocene (Brule Formation) and Eocene (Chadron Formation) fossils from strata in South Dakota, Nebraska, and Wyoming to identify and compare patterns of preservation in fossils from different geologic ages, depositional environments, and paleoclimatic regimes. All fossils used in this study were collected and analyzed as part of an earlier effort to determine the role(s) of rare earth elements (REE) in bone fossilization and the applicability of REE fingerprinting as a method to deter fossil poaching on federal lands (see [17–19]). Individual sites were chosen based on geologic age, lithology, and known frequency of poaching activities from personal observations and/or as informed by Badlands National Park staff.

## 2. Background

### 2.1. Cellular and Soft Tissue Preservation in Vertebrate Fossils

Over the last decade, there has been an increasing amount of research concerning the context and controls on soft tissue and cellular preservation in fossil vertebrates. Osteocytes and blood vessels have been recovered from a variety of skeletal elements, vertebrate taxa, and depositional environments (marine, freshwater, and terrestrial) from Mesozoic and Cenozoic fossils (e.g., [8,12,15,16]). Bone size also does not appear to be a major controlling factor, as endogenous proteins have been recovered from both large and small skeletal elements (e.g., [20,21]). Researchers have also begun to investigate mineralogical and diagenetic factors involved in soft tissue preservation (e.g., [22]). One study found that iron minerals played an important role in bone cell preservation, forming iron oxide pseudomorphs as a result of early diagenetic reactions [23]. It has also been suggested that soft tissues are more likely to preserve in oxidizing depositional environments [10]—such depositional environments are well-represented in the White River Group, including floodplain, aggradational eolian, stable eolian, lacustrine, forested, and open, lightly vegetated environments [4,24]. In contrast, soft tissues in fossil specimens have been recovered from reducing depositional environments [11,25], possibly stemming from rapid burial in iron-rich sediments.

Following death and significant decay of ultrastructural soft tissues (i.e., muscles and adipose tissues), vertebrate bones recrystallize to become carbonate hydroxy-fluorapatite. During the process of fossilization, the organic components of bone tissue (i.e., osteocytes, blood vessels, fibrous matrix) and the biomolecules comprising them may be damaged or entirely lost as a result of diagenesis. Bioapatite has a very low crystallinity (small crystallite size) during life, but during fossilization its crystallinity increases [26,27]. The extent of recrystallization and homogeneity of hydroxyapatite crystal size in fossil bone is determined by the Crystallinity Index, which can be used to investigate diagenetic effects on fossil bone [28]. An inverse relationship between the degree of crystallinity of a fossil bone and the amount of organic material preserved within it has been noted [28]. Similarly, a correlation between fossil bone apatite crystallinity and trace element uptake was noted [29], with the suggestion that fast recrystallization rates (as inferred from trace element concentration profiles) may facilitate long-term retention of endogenous microstructures and their constituent biomolecules.

### 2.2. Sedimentology of the White River Group

The lowermost units of the White River Group (Chamberlain Pass and Chadron Formations) primarily consist of extensive fluvial channel sandstones and floodplain paleosols altered by the humid late Eocene climate and expressed as colorful bands of strata in parts of the White River Badlands [30,31]. In contrast, the Oligocene Brule Formation is composed of brown and tan mudstones gradually giving way to tan siltstones higher up-section [4], indicating a transition from subhumid to subarid conditions (Figure 2). Volcanic materials sourced from Nevada and Utah were transported east and are found throughout the White River Group [24]. Lower in the section, volcanic material was mixed with alluvial sediments derived from the Black Hills to form the Chamberlain Pass Formation, up through the Scenic Member of the Brule Formation. Higher in the section, volcanic materials were deposited as dryland loess, as commonly seen in the thick siltstone layers of the upper Poleslide Member of the Brule Formation [4,24].

### 2.3. Stratigraphic and Paleopedological Context of the Sharps Formation

The Sharps Formation overlies the Upper Poleslide Member of the Brule Formation (Figure 3), which is the highest (currently) recognized unit within the White River Group, with a distinctive white layer (commonly referred to as the Rockyford Ash) separating the two rock units. While the Sharps Formation and Rockyford Ash are currently regarded as the lowest units of the Arikaree Group, the Sharps Formation and Upper Poleslide Member of the Brule Formation appear to be lithologically identical (Figure 2), with both units containing tan and brown, silty sandstone and sandy siltstone beds [4]. The similarity

between the uppermost White River Group siltstone beds and the Sharps Formation led earlier researchers to conclude that the two are equivalent [32]. This distinctive white layer in the Cedar Pass area of Badlands National Park is not an ash bed, but instead a mixture of weathered volcanic materials and epiclastic debris that does not correlate with the true Rockyford Ash at the base of the Sharps Formation on Sheep Mountain Table near Rockyford, South Dakota [4]. We follow the nomenclature of [4] and refer to this distinctive bed as the *Cedar Pass white layer* and use it as a stratigraphic reference point throughout this study. Formal revision of the stratigraphic nomenclature of the Brule vs. Sharps Formations has yet to be published, and as such we refer to the strata above the Cedar Pass white layer as the Sharps Formation, although they are identical to strata within the underlying Poleslide Member of the Brule Formation.

In the Poleslide Member, massive siltstone beds are interpreted as volcaniclastic loess deposits, whereas sandstones represent stream deposits; the strata of the Sharps Formation are interpreted to have very similar origins based on their similar lithologies and overall geomorphic expression [4,30]. In terms of paleopedology, a shift is observed from forest soils (alfisols) at the base of the Brule Formation (which includes both the Scenic Member and the Poleslide Member) to grassland soils (mollisols), which formed within with fluvial, lacustrine, and eolian environments, each trading prominence throughout the Poleslide Member [4,30].

## 3. Methods

### 3.1. Field Collection

Vertebrate fossil specimens of large, postcranial bones (including tortoise carapace fragments) were collected in situ from each major depositional environment within the Sharps Formation (channel sandstones, stable floodplain environments, and aggradational eolian environments) in the Cedar Pass area of Badlands National Park, generating a total of eight specimens (Figures 4 and 5). The stratigraphic position and preservational attributes (e.g., fracturing, color) of specimens were noted in order to place each specimen into temporal context and to interpret its taphonomic history. Seven fossil bones previously collected from channel and floodplain deposits within the underlying White River Group (Chadron and Brule formations) were also analyzed for comparison with the new fossils from the Sharps Formation (Figure 3).
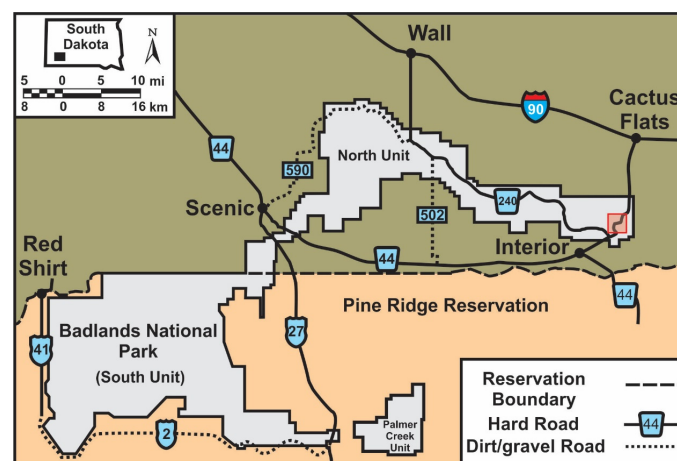


**Figure 4.** Map of Badlands National Park in South Dakota, USA. The study area where the fossil specimens examined in this study were collected is highlighted by the red box. Modified from [31].
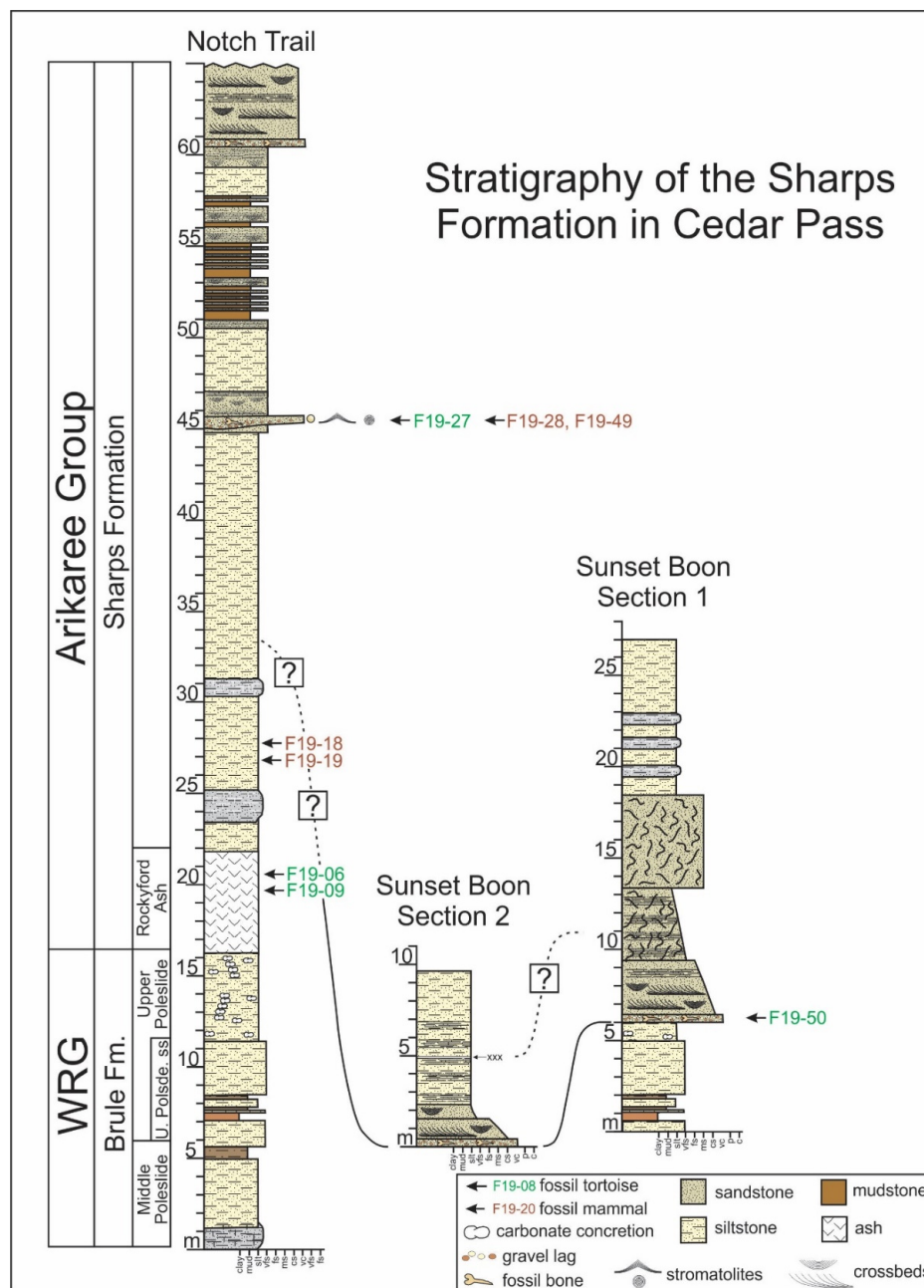
**Figure 5.** Stratigraphic section of the Sharps Formation in the Cedar Pass area of Badlands National Park, SD, USA. Elevations of sample locations are located on the left side of each column and locality names for each section are labeled on the top of each respective section. "F19-##" denotes field numbers for fossil specimens. Note that the Rockyford Ash is equivalent to the *Cedar Pass white layer* [4].

*3.2. Demineralization and Soft Tissue Analysis*

Fragments of bone material were demineralized following established protocols [11]. Roughly 0.5 cm$^3$ fragments of each specimen were demineralized in 0.22 μm filtered 0.5 M Ethylenediaminetetraacetic acid (EDTA) at pH 8 in polystyrene cell culture plates. Demineralization occurred over 2–6 weeks, with the EDTA solution replaced approximately every 48 h. Demineralization products were then drawn from the culture plates with sterile pipettes, placed on glass slides, and capped by a glass cover slip. Any isolated soft tissue or cellular structures were identified via standard (transmitted light) optical microscopy, with identifications based on morphologic consistency with counterpart cells/tissues

from extant vertebrates (e.g., [11,15]). As negative controls, sediment samples from the four collection localities in the Sharps Formation (Rockyford Ash, lower siltstone bed, and upper channel sandstone) were also demineralized and examined following the same protocols used with the fossil specimens. Images of demineralization products (both from the fossils and sediment controls) were captured using a Nikon Eclipse microscope equipped with a Nikon DSFi-3 camera and NIS Elements software (Nikon, Tokyo, Japan).

Patterns of soft tissue and cellular preservation were compared between individual vertebrate fossils and cross-referenced with associated sedimentological data from strata lower in the White River Group [18,33–38]. This permitted a comprehensive analysis of the transition from late Eocene paleoenvironments (humid and forested fluvial channels and floodplains) to those of the early and middle Oligocene (open, eolian dominated savannah conditions) with respect to any potential influence of each paleoclimatic/paleoenvironmental regime on soft tissue and cellular preservation.

### 3.3. Thin Section Preparation and Microscopy

Following standard techniques (e.g., [39]), a fragment of each fossil was cut using a Buehler Isomet diamond trim saw, mounted on a glass slide with epoxy, polished with fine (600 μm) silicon carbide grit, and imaged in both cross-polarized and transmitted light microscopy. Features of interest included Haversian canals in the cortical bone based on comparisons to earlier work [40], as well as secondary mineral infills in cavities, which were interpreted based on crystal morphologies to infer associated paleoclimatic and diagenetic conditions documented in previous studies (e.g., [41,42]).

### 3.4. Mineralogy and Crystallinity Analysis

Mineralogy and crystallinity of fossil vertebrate specimens were determined by X-ray diffraction (XRD). Preparation of the fossils for XRD analysis followed existing techniques [29]. Specifically, a fragment of each fossil was cleaned with hand tools to remove excess sediment before being ground into a powder with a mortar and pestle. Each fossil powder was then filtered through a sieve (63 μm mesh) to acquire grains of uniform size. The fossil powders were analyzed using a Bruker D8 Advance powder X-ray diffraction system, fitted with a rotating stage and a copper K$\alpha$ radiation tube set to 40 kV and 40 mA, scanning a 2θ range of 0° to 70° in a continuous mode. Each fossil was then assigned a hydroxyapatite Crystallinity Index (CI) value [28].

## 4. Results

### 4.1. Demineralization Products and Bone Apatite Crystallinity

All demineralized fossils yielded microstructures matching the morphology of vertebrate blood vessels and fibrous proteinaceous bone matrix, and all but four of the specimens preserved structures consistent in morphology with vertebrate osteocytes (Table 1). These microstructures were recovered from all fossils regardless of geologic age, skeletal element, host lithology, and source taxon. Of the four fossils that did not yield osteocytes, two were tortoises and two were mammals, two were Oligocene in age while two were from late Eocene strata, two were from fluvial channel sandstones, and one each from a floodplain mudstone and eolian siltstone. Fragments of extracellular matrix were identified by their fibrous texture (Figure 6A–C), while blood vessel fragments were recognized by their tubular, branching forms and hollowness (Figure 6D–G), and osteocytes were identifiable either individually as small (generally no more than 20 μm in length), prolate structures with thin, branching extensions consistent in form with cellular filopodia (Figure 6H,I), or in groups clustered together within partially demineralized bone matrix (Figure 6J–L). Demineralization of associated sediment samples (Figure 7) yielded small masses of argillaceous material and silt-size quartz grains but no identifiable organic microstructures.

**Table 1.** Summary of soft tissue and cellular microstructures recovered from demineralization of each fossil, including crystallinity index (CI) values for each specimen [28]. Abbreviation: indet.: indeterminate.

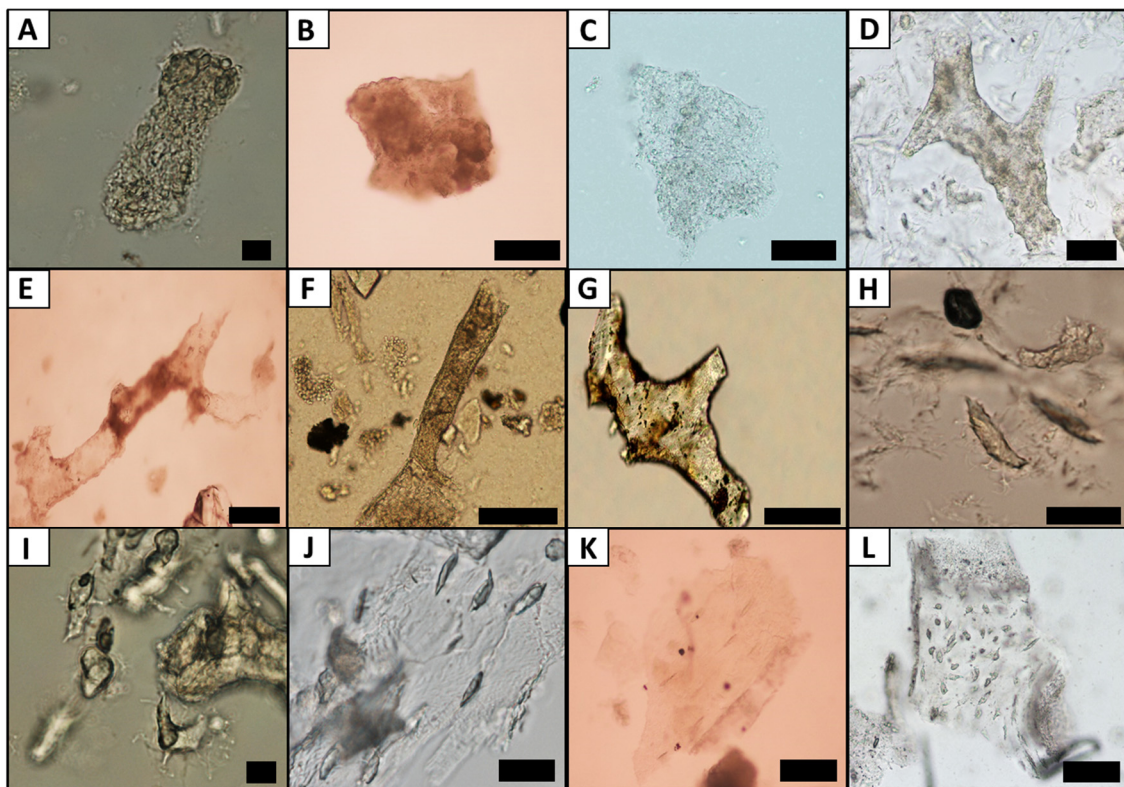| Specimen | Taxon | Age | Element | Lithology | Osteocytes | Blood Vessels | Fibrous Matrix | CI Value |
|----------|-------|-----|---------|-----------|------------|---------------|----------------|----------|
| F19-50 | Tortoise | Oligocene | Shell | Channel Sandstone | Absent | Uncommon | Rare | 0.42 |
| F19-49 | Mammal | Oligocene | Indet. postcranial | Channel Sandstone | Rare | Frequent | Rare | 0.42 |
| F19-28 | Mammal | Oligocene | Indet. Rib | Channel Sandstone | Rare | Uncommon | Rare | 0.42 |
| F19-27 | Tortoise | Oligocene | Shell | Channel Sandstone | Abundant | Uncommon | Rare | 0.43 |
| F19-24 | Tortoise | Oligocene | Shell | Volcanic Ash | Abundant | Frequent | Rare | 0.50 |
| F19-19 | Carnivore | Oligocene | Ulna | Eolian Siltstone | Absent | Uncommon | Rare | 0.46 |
| F19-18 | Oreodont | Oligocene | Rib | Eolian Siltstone | Rare | Uncommon | Rare | 0.51 |
| F19-10 | Mammal | Oligocene | Indet. rib | Eolian Siltstone | Abundant | Abundant | Rare | 0.40 |
| F19-9 | Tortoise | Oligocene | Shell | Volcanic Ash | Rare | Rare | Rare | 0.43 |
| F19-8 | Tortoise | Oligocene | Shell | Volcanic Ash | Uncommon | Uncommon | Frequent | 0.53 |
| F19-7 | Tortoise | Oligocene | Shell | Eolian Siltstone | Rare | Abundant | Absent | 0.48 |
| F19-6 | Tortoise | Oligocene | Shell | Volcanic Ash | Abundant | Uncommon | Rare | 0.60 |
| F19-3 | Tortoise | Oligocene | Shell | Eolian Siltstone | Absent | Abundant | Absent | 0.52 |
| F19-1 | Mammal | Oligocene | Indet. limb Bone | Eolian Siltstone | Absent | Absent | Absent | 0.53 |
| F101 | Tortoise | Oligocene | Shell | Eolian Siltstone | Abundant | Frequent | Abundant | 0.36 |
| F47 | Tortoise | Oligocene | Shell | Floodplain Mudstone | Abundant | Frequent | Frequent | 0.28 |
| F12-70 | Tortoise | Eocene | Shell | Floodplain Mudstone | Abundant | Uncommon | Uncommon | 0.44 |
| F15 | Mammal | Eocene | Indet. Limb | Floodplain Mudstone | Abundant | Uncommon | Rare | 0.32 |
| FR09-09 | Mammal | Eocene | Indet. Rib | Floodplain Mudstone | Rare | Rare | Uncommon | 0.46 |
| F08-87 | Tortoise | Eocene | Shell | Channel Sandstone | Absent | Frequent | Rare | 0.44 |
| F08-80 | Brontothere | Eocene | Rib | Floodplain Mudstone | Abundant | Abundant | Frequent | 0.61 |
| F08-77 | Oreodont | Eocene | Stylopodial | Floodplain Mudstone | Absent | Uncommon | Rare | 0.65 |
| F08-10 | Brontothere | Eocene | Rib | Floodplain Mudstone | Frequent | Abundant | Uncommon | 0.43 |
| F08-09 | Brontothere | Eocene | Femur | Floodplain Mudstone | Abundant | Abundant | Frequent | 0.47 |
| F08-08 | Brontothere | Eocene | Indet. Metapodial | Floodplain Mudstone | Uncommon | Abundant | Frequent | 0.37 |
| F08-915-R | Brontothere | Eocene | Scapula | Floodplain Mudstone | Rare | Abundant | Uncommon | 0.47 |

**Figure 6.** Photomicrographs of demineralization products from White River Group fossil specimens. (**A**–**C**) Fibrous matrix fragments from tortoise shells ((**A**) F19-50 and (**C**) F101) and a mammal limb bone ((**B**) F08-77). (**D**–**G**) Branching, hollow structures identified as blood vessel fragments ((**D**) F47, Tortoise shell; (**E**) F08-87, Tortoise shell; (**F**) F19-18, Mammal rib; (**G**) F19-28, Mammal rib). (**H,I**) Individual osteocytes with branching filopodia ((**H**) F47, Tortoise shell; (**I**) F19-06, Tortoise shell). (**J**–**L**) Small, prolate osteocytes in partially demineralized bone matrix ((**J**) F15, Mammal limb bone; (**K**) FR09-09, Mammal rib; (**L**) F101, Tortoise shell). Scale bars equal 10 µm in (**A,I**), 25 µm in (**H,J**), 50 µm in (**B**–**D,K**), and 100 µm in (**E**–**G,L**).



**Figure 7.** Photomicrographs of demineralization products from White River Group sediment samples. (**A**) Sediment from the Rockyford Ash/Cedar Pass white layer. (**B**) Eolian siltstone sample (stratigraphically equivalent to fossils F19-18 and F19-19). (**C**) A fluvial channel sandstone (stratigraphically equivalent to F19-50). As shown in these images, only silt-sized quartz grains and minute aggregates of argillaceous sediment (darker masses in (**B,C**)) were encountered in the sediment samples.

Apatite crystallinity was also examined to assess the relationship between diagenetic recrystallization of bioapatite and extent of soft tissue preservation (Table 1). CI values were found to vary from 0.28 to 0.65, with no clear pattern in relation to the recovery of any

of the three microstructures examined (Table 1). There is no significant difference between Eocene and Oligocene fossils. Although the sample size was small, there was no significant difference in CI values between fossils with and without osteocytes. However, calcite was absent in most fossils in which osteocytes were also absent.

### 4.2. Bone and Secondary Mineral Micromorphology and Diagenetic History

Thin sections of many of the fossil specimens revealed well-preserved microstructural preservation of extensive Haversian canal systems, especially in the external cortex (Figure 8A–C), with primary osteons, secondary osteons, and individual osteocyte lacunae each still clearly visible. Several specimens contained elongate or circular features representing resorption cavities (e.g., Figure 8D–G). Virtually all such cavities were infilled with calcite, which was primarily sparry in form (Figure 8D–F). Specimen F19-06 contained iron oxide as well, usually clustered around the edges of cavities, with sparry calcite forming a second-generation infilling cement that occupied the rest of the space (Figure 8E,F). In this specimen, iron oxide tended to most often be found on one side of larger cavities, presumably representing "spirit-level" secondary mineral deposits formed on the quarry-down side within these larger spaces (cf., [43]; Figure 8F), but in smaller cavities it was typically found to coat the entire perimeter (Figure 8E). Some fossils (F47, F101, and F19-28) possess thin micritic calcite linings on the walls of cavities which are then infilled by sparry calcite. Specimens F19-19 and F19-50 generally exhibit poorly preserved bone texture, with fine histologic structures (i.e., osteons, lines of arrested growth) within the cortex largely altered via microbial attack/bioerosion and apparent recrystallization (cf., [44]; Figure 8G–I).
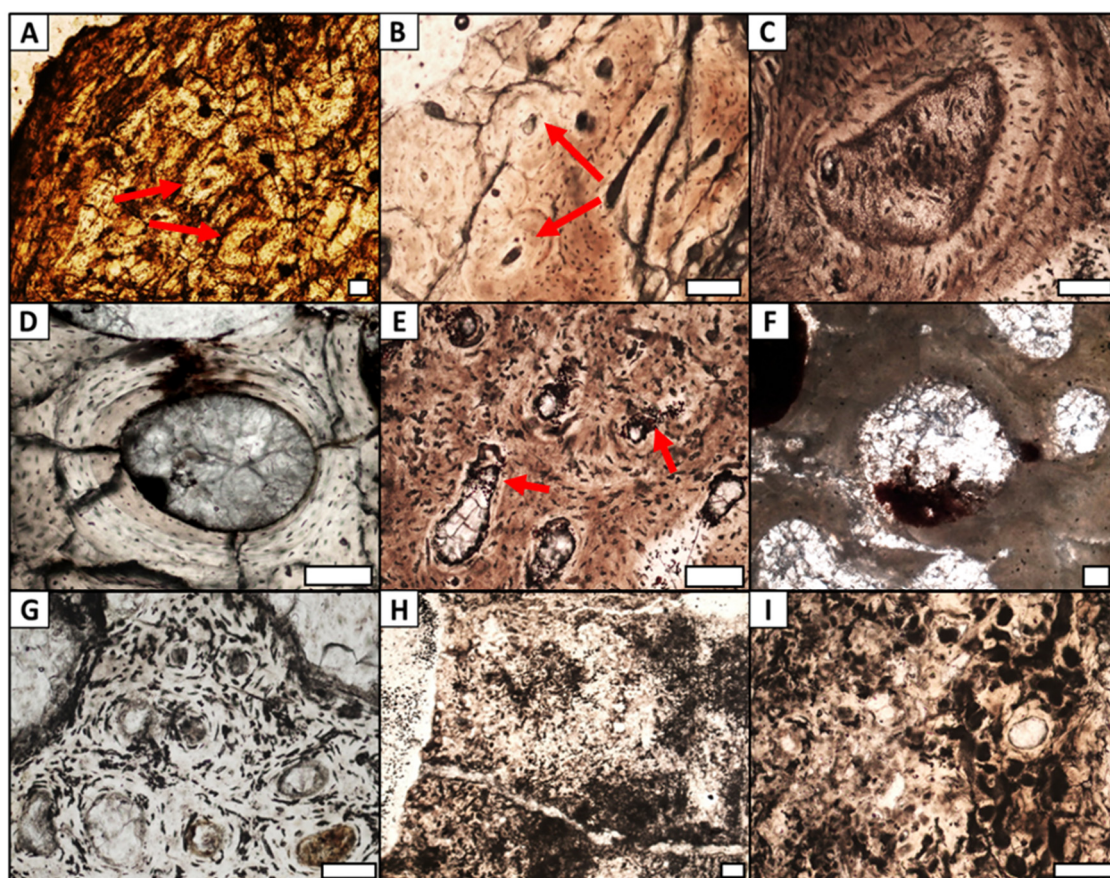


**Figure 8.** Photomicrographs of thin sections of the White River Group fossil specimens. (**A**) Haversian systems (red arrows) in the external cortex of a mammal limb bone (Specimen F15). (**B**) Haversian systems (red arrows) in the external cortex of a mammal rib (FR09-09). (**C**) Close-up of osteons and osteocytes in the cortical bone of a tortoise shell (F19-06). (**D**) Sparry calcite

infilling of a cavity in a mammal rib (F19-28). (**E**) Red, polygonal iron oxide particles (red arrows) in a tortoise shell bone (F19-06). (**F**) Iron oxide accumulation at the "bottom" of a large cavity infill (F19-06). (**G**) Well-preserved osteons and Haversian systems within the outer cortex of a tortoise shell (F19-50). (**H,I**) Poorly preserved bone histology in the external cortex of a mammal ulna (F19-19). Scale bars equal 100 μm in all panels.

## 5. Discussion

### 5.1. Trends in Soft Tissue Preservation

While all fossil specimens examined were found to retain organic microstructures (vessels and fibrous matrix fragments), considerable variation was encountered in terms of the abundance and quality of osteocyte preservation. Fossils with poorly preserved histology in the thin section (e.g., Figure 8H,I) did not yield any identifiable osteocytes after demineralization, indicating that the apparent pattern in osteocyte preservation in Table 1 corresponds to the extent of diagenetic alteration. Intriguingly, this finding parallels a recent trend identified in fossil bones preserved in shallow marine environments [25], indicating that there are commonalities to bone decay among disparate depositional environments which, in turn, impart similar outcomes in terms of cellular and soft tissue preservation.

The most surprising finding in this study was the great prevalence of soft tissue and cellular preservation within the specimens, particularly of vessels and fibrous matrix fragments (Table 1). Recovery of these microstructures across all taxa, depositional environments, skeletal elements, and geologic ages supports the interpretation that organic microstructure preservation may be independent of these factors (e.g., [9,12,15,16,45]. However, the fact that endogenous microstructures were recovered from all fossils, regardless of taxonomy, host lithology and depositional environment, remains unexpected given conventional wisdom and historical hypotheses. In contrast, recent research suggests that the type of fossil bone (compact vs. cancellous) preserves different apatite crystallinity values that may correlate to the type of soft tissue preserved, that taxonomy shows a correlation with the type of soft tissue that is preserved, and that biomechanical function shows no correlation with soft tissue preservation [46,47].

Regardless, when placed in context with other recent studies (e.g., [12,25]), our results suggest that preservation of soft tissue and cellular microstructures may be more common in fossil bones than previously thought.

### 5.2. Bone Histology and Post-Depositional Conditions

Of the three fossil specimens that exhibited poorly preserved bone histology (F08-77, F19-19, and F19-50), all were from different depositional environments and ages. The only shared trait was their lack of identifiable osteocytes in the thin section. Hence, the poor histological and cellular preservation observed in these three fossils is more likely a result of individual diagenetic alteration rather than shared climatic or environmental conditions at the time of fossilization.

In all fossils with calcite infills (F47, F101, F19-06, F19-18, F19-28, and F19-50), equant and blocky morphologies were dominant (e.g., Figure 8D–F). The prevalence of sparry, diagenetic calcite is notable, especially in the Oligocene fossils collected from eolian siltstones (e.g., F19-18), since calcite of this form is indicative of saturated or phreatic diagenetic conditions [41,42]. The sparry calcite cavity infills are likely the result of post-depositional phreatic saturation since their depositional environments have been interpreted as dry [4,30,33]. The Eocene fossils, in contrast, either lacked any clear cavity infill or exhibited micrite instead of more crystalline, sparry calcite (e.g., F08-87). Micritic calcite is indicative of vadose conditions [41,42]; the presence of micrite lining the cavity walls around the centrally located sparry calcite in some fossils (F47, F101, and F19-28) implies a relatively dry, unsaturated setting followed by phreatic saturation after burial. The presence of iron oxide in F19-06 suggests oxidizing conditions, though this too may be reflective of diagenetic redox conditions instead of those of the initial depositional environment. The

apparent lack of iron in the cells, vessels, and fibrous matrix fragments contrasts with the findings of previous studies (e.g., [7,9,11]), which identified a connection between iron-rich sediments and endogenous microstructure preservation. Thus, cellular and soft tissue microstructure preservation may not always be reliant on diagenetic iron mineralization, as some authors have suggested (e.g., [23]).

## 6. Conclusions

This study is among the first to examine the influences of a broad range of factors on soft tissue and cellular preservation in fossil bones, including geologic age, depositional environment, and paleoclimatic conditions. Neither taxonomic identity, host lithology, nor paleoclimatic regime (e.g., warm and humid Eocene vs. cooler and drier Oligocene) were found to influence soft tissue or cellular recovery. These findings, in combination with the observed prevalence and morphologic integrity of the tissue and cellular structures documented in this study, suggest that these endogenous microstructures may not be as rare in fossil bones as historically thought.

Future studies on this topic are clearly warranted, with special attention toward diagenetic factors, such as metamorphic history, chemical alteration, and trace element uptake. Incorporating additional, complementary methods of analysis such as cathodoluminescence and scanning electron microscopy in conjunction with energy dispersive X-ray spectroscopy could also be used to corroborate and refine observations and interpretations from thin-section petrography and optical microscopy, thereby providing a more complete picture of post-depositional conditions and diagenetic history. Multidisciplinary studies of fossil specimens from diverse depositional environments offer the most informative path forward to discerning the relative importance of large-scale/external (i.e., climatic, geologic) versus small-scale/internal (i.e., redox, pH) conditions as controls on soft tissue and biomolecular preservation in the fossil record.

# References

1. Terry, D.O., Jr. Paleopedology of the Chadron Formation of Northwestern Nebraska: Implications for paleoclimatic change in the North American midcontinent across the Eocene–Oligocene boundary. *Palaeogeogr. Palaeoclimatol. Palaeoecol.* **2001**, *168*, 1–38. [CrossRef]
2. Prothero, D.R.; Emry, R.J. *The Terrestrial Eocene-Oligocene Transition in North America*; Cambridge University Press: New York, NY, USA, 2005; 708p.
3. Zanazzi, A.; Kohn, M.J.; MacFadden, B.J.; Terry, D.O. Large temperature drop across the Eocene–Oligocene transition in central North America. *Nature* **2007**, *445*, 639. [CrossRef] [PubMed]
4. Benton, R.C.; Terry, D.O., Jr.; Evanoff, E.; McDonald, H.G. *The White River Badlands: Geology and Paleontology*; Indiana University Press: Bloomington, IN, USA, 2015; 222p.
5. Terry, D.O., Jr. Stratigraphy, depositional environments, and fossil resources of the Chadron Formation in the South Unit of Badlands National Park, South Dakota. In *Partners Preserving our Past, Planning our Future: Proceedings for the Fifth Conference on Fossil Resources, Dakoterra*; Martin, J.E., Hoganson, J.W., Benton, R.C., Eds.; South Dakota School of Mines & Technology: Rapid City, SD, USA, 1998; Volume 5, pp. 127–138.
6. Schweitzer, M.H.; Wittmeyer, J.L.; Horner, J.R.; Toporski, J.K. Soft-tissue vessels and cellular preservation in *Tyrannosaurus rex*. *Science* **2005**, *307*, 1952–1955. [CrossRef] [PubMed]
7. Schweitzer, M.H.; Wittmeyer, J.L.; Horner, J.R. Soft tissue and cellular preservation in vertebrate skeletal elements from the Cretaceous to the present. *Proc. R. Soc. B Biol. Sci.* **2007**, *274*, 183–197. [CrossRef] [PubMed]
8. Bertazzo, S.; Maidment, S.C.; Kallepitis, C.; Fearn, S.; Stevens, M.M.; Xie, H.N. Fibres and cellular structures preserved in 75-million–year-old dinosaur specimens. *Nat. Commun.* **2015**, *6*, 7352. [CrossRef] [PubMed]
9. Cadena, E.A. Microscopical and elemental FESEM and Phenom ProX-SEM-EDS analysis of osteocyte- and blood vessel-like microstructures obtained from fossil vertebrates of the Eocene Messel Pit, Germany. *PeerJ* **2016**, *4*, e1618. [CrossRef] [PubMed]
10. Wiemann, J.; Fabbri, M.; Yang, T.R.; Stein, K.; Sander, P.M.; Norell, M.A.; Briggs, D.E. Fossilization transforms vertebrate hard tissue proteins into N-heterocyclic polymers. *Nat. Commun.* **2018**, *9*, 4741. [CrossRef] [PubMed]
11. Ullmann, P.V.; Pandya, S.H.; Nellermoe, R. Patterns of soft tissue and cellular preservation in relation to fossil bone tissue structure and overburden depth at the Standing Rock Hadrosaur site, Maastrichtian Hell Creek Formation, South Dakota, USA. *Cretac. Res.* **2019**, *99*, 1–13. [CrossRef]
12. Ullmann, P.V.; Schweitzer, M.H. A statistical meta-analysis of lithologic and other potential controls on fossil bone cellular and soft tissue preservation. *Palaios* **2023**, *38*, 246–257. [CrossRef]
13. Schweitzer, M.H.; Zheng, W.; Cleland, T.; Bern, M. Molecular analyses of dinosaur osteocytes support the presence of endogenous molecules. *Bone* **2013**, *52*, 414–423. [CrossRef]
14. Cleland, T.P.; Schroeter, E.R.; Zamdborg, L.; Zheng, W.; Lee, J.E.; Tran, J.C.; Bern, M.; Duncan, M.B.; Lebleu, V.S.; Ahlf, D.R.; et al. Mass spectrometry and antibody-based characterization of blood vessels from *Brachylophosaurus canadensis*. *J. Proteome Res.* **2015**, *14*, 5252–5262. [CrossRef] [PubMed]
15. Cadena, E.A.; Schweitzer, M.H. Variation in osteocytes morphology vs bone type in turtle shell and their exceptional preservation from the Jurassic to the present. *Bone* **2012**, *51*, 614–620. [CrossRef] [PubMed]
16. Cadena, E.A.; Schweitzer, M.H. A pelomedusoid turtle from the Paleocene-Eocene of Colombia exhibiting preservation of blood vessels and osteocytes. *J. Herpetol.* **2014**, *48*, 461–465. [CrossRef] [PubMed]
17. Grandstaff, D.E.; Terry, D.O., Jr. Rare earth element composition of Paleogene vertebrate fossils from Toadstool Geologic Park, Nebraska, USA. *Appl. Geochem.* **2009**, *24*, 733–745. [CrossRef]
18. Terry, D.O., Jr.; Grandstaff, D.E.; Cerruti, A.D.; Lalor, E.F.; Lukens, W.E. Regional variability of geochemical signatures in fossils from the Paleogene White River Sequence of South Dakota, Nebraska, and Wyoming. In Proceedings of the 10th Conference on Fossil Resources, Dakoterra, Rapid City, SD, USA, 13–15 May 2014; Volume 6, pp. 73–75.
19. Terry, D.O., Jr.; Grandstaff, D.E. The nonmarine Eocene-Oligocene climate transition of the northern Great Plains, USA: Insights from rare earth element signatures of fossil bone. In Proceedings of the 3rd International Paleontological Congress, London, UK, 28 June–3 July 2010; p. 374.
20. Schweitzer, M.H.; Zheng, W.; Organ, C.L.; Avci, R.; Suo, Z.; Freimark, L.M.; Lebleu, V.S.; Duncan, M.B.; Heiden, M.G.V.; Neveu, J.M.; et al. Biomolecular characterization and protein sequences of the Campanian hadrosaur *B. canadensis*. *Science* **2009**, *324*, 626–631. [CrossRef] [PubMed]
21. Lindgren, J.; Uvdal, P.; Engdahl, A.; Lee, A.H.; Alwmark, C.; Bergquist, K.E.; Nilsson, E.; Ekström, P.; Rasmussen, M.; Douglas, D.A.; et al. Microspectroscopic evidence of Cretaceous bone proteins. *PLoS ONE* **2011**, *6*, e19445. [CrossRef] [PubMed]
22. Boatman, E.M.; Goodwin, M.B.; Holman, H.-Y.; Fakra, S.; Zheng, W.; Gronsky, R.; Schweitzer, M.H. Mechanisms of soft tissue and protein preservation in *Tyrannosaurus rex*. *Sci. Rep.* **2019**, *9*, 15678. [CrossRef] [PubMed]
23. Surmik, D.; Dulski, M.; Kremer, B.; Szade, J.; Pawlicki, R. Iron-mediated deep-time preservation of osteocytes in a Middle Triassic reptile bone. *Hist. Biol.* **2019**, *33*, 186–193. [CrossRef]

24. Larson, E.E.; Evanoff, E. *Depositional Environments, Lithostratigraphy, and Biostratigraphy of the White River and Arikee Groups (Late Eocene to Early Miocene, North America)*; Geological Society of America Special Paper; Geological Society of America: Boulder, CO, USA, 1998; p. 325.

25. Voegele, K.K.; Ullmann, P.V.; Boles, Z.M.; Schroeter, E.R.; Zheng, W.; Schweitzer, M.H.; Lacovara, K.J. Soft tissue and biomolecular preservation in vertebrate fossils from glauconitic, shallow marine sediments of the Hornerstown Formation, Edelman Fossil Park, New Jersey. *Biology* **2022**, *11*, 1161. [CrossRef]

26. Hubert, J.F.; Panish, P.T.; Chure, D.J.; Prostak, K.S. Chemistry, microstructure, petrology, and diagenetic model of Jurassic dinosaur bones, Dinosaur National Monument, Utah. *J. Sediment. Res.* **1996**, *66*, 531–547.

27. Elorza, J.; Astibia, H.; Murelaga, X.; Pereda-Suberbiola, X. Francolite as a diagenetic mineral in dinosaur and other Upper Cretaceous reptile bones (Lano, Iberian Peninsula): Microstructural, petrological and geochemical features. *Cretac. Res.* **1999**, *20*, 169–187. [CrossRef]

28. Person, A.; Bocherens, H.; Saliège, J.F.; Paris, F.; Zeitoun Gérard, M. Early diagenetic evolution of bone phosphate: An X-ray diffractometry analysis. *J. Archaeol. Sci.* **1995**, *22*, 211–221. [CrossRef]

29. Trueman, C.N.; Palmer, M.R.; Field, J.; Privat, K.; Ludgate, N.; Chavagnac, V.; Eberth, D.A.; Cifelli, R.; Rogers, R.R. Comparing rates of recrystallisation and the potential for preservation of biomolecules from the distribution of trace elements in fossil bones. *Comptes Rendus Palevol* **2008**, *7*, 145–158. [CrossRef]

30. Retallack, G.J. *Late Eocene and Oligocene paleosols from Badlands National Park, South Dakota*; Geological Society of America Special Paper; Geological Society of America: Boulder, CO, USA, 1983; p. 193.

31. Terry, D.O., Jr.; Evans, J.E. Pedogenesis and paleoclimatic implications of the Chamberlain Pass Formation, basal White River Group, badlands of South Dakota. *Palaeogeogr. Palaeoclimatol. Palaeoecol.* **1994**, *110*, 197–215. [CrossRef]

32. Tedford, R.H.; Swinehart, J.B.; Hunt, R.M.; Voorhies, M.R. Uppermost White River and lowermost Arikaree rocks and faunas, White River Valley, northwestern Nebraska, and their correlation with South Dakota. Fossiliferous Cenozoic deposits of western South Dakota and northwestern Nebraska. *Mus. Geol. South Dak. Sch. Mines Technol. Dakoterra* **1985**, *2*, 335–352.

33. Mintz, J.S.; Terry, D.O., Jr.; Stinchcomb, G. The Terrestrial Response to the Post Eocene-Oligocene Climatic Transition, Poleslide Member, Brule Formation, Badlands National Park, South Dakota. *Geol. Soc. Am. Abstr. Programs* **2007**, *39*, 193.

34. Stinchcomb, G.; Terry, D.O., Jr.; Mintz, J.S. Paleosols and stratigraphy of the Scenic-Poleslide Member boundary: Implications for pedofacies analysis and regional correlation of the early Oligocene Brule Formation, South Dakota, USA. *Geol. Soc. Am. Abstr. Programs* **2007**, *39*, 305.

35. Griffis, N.; Terry, D.O., Jr. Vertical changes in paleosol morphology within the White River Sequence at Flagstaff Rim, Wyoming: Implications for paleoclimatic change leading up to the Eocene-Oligocene Transition. *Geol. Soc. Am. Abstr. Programs* **2010**, *42*, 20.

36. Cerruti, A.D.; Terry, D.O., Jr.; Grandstaff, D.E. Geochemical Analysis of Fossil Bone from Badlands National Park: A Test of the Rare Earth Element Fingerprinting Method to Combat Fossil Poaching. In Proceedings of the 10th Conference on Fossil Resources, Dakoterra, Rapid City, SD, USA, 13–15 May 2014; Volume 6, pp. 34–36.

37. Lalor, E.F.; Terry, D.O., Jr.; Grandstaff, D.E.; Cerruti, A.D. The use of nondestructive X-ray fluorescence as a forensic tool for geochemically fingerprinting fossil resources. In Proceedings of the 10th Conference on Fossil Resources, Dakoterra, Rapid City, SD, USA, 13–15 May 2014; 2014; Volume 6, pp. 50–52.

38. Conwell, C.T.; Terry, D.O., Jr.; Tumarkin-Deratzian, A.R.; Grandstaff, D.E. From bone to stone: The influence of depositional environments on the fossilization of vertebrate bone from the Paleogene White River Group, Badlands National Park, South Dakota. *Geol. Soc. Am. Abstr. Programs* **2016**, *48*. [CrossRef]

39. Lamm, E.T. Preparation and Sectioning of Specimens. In *Bone Histology of Fossil Tetrapods: Advancing Methods, Analysis, and Interpretation*; Padian, K., Lamm, E.T., Eds.; University of California Press: Berkeley, CA, USA, 2013; pp. 55–160.

40. Garland, A.N. Microscopical analysis of fossil bone. *Appl. Geochem.* **1989**, *4*, 215–229. [CrossRef]

41. Khormali, F.; Abtahi, A.; Stoops, G. Micromorphology of calcitic features in highly calcareous soils of Fars Province, Southern Iran. *Geoderma* **2006**, *132*, 31–46. [CrossRef]

42. Tófalo, O.R.; Pazos, P.J. Paleoclimatic implications (Late Cretaceous–Paleogene) from micromorphology of calcretes, palustrine limestones and silcretes, southern Paraná Basin, Uruguay. *J. South Am. Earth Sci.* **2010**, *29*, 665–675. [CrossRef]

43. Pfretzschner, H.-U.; Tütken, T. Rolling bones—Taphonomy of Jurassic dinosaur bones inferred from diagenetic microcracks and mineral infillings. *Palaeogeogr. Palaeoclimatol. Palaeoecol.* **2011**, *310*, 117–123. [CrossRef]

44. Jans, M.M.E. Microbial bioerosion of bone—A review. In *Current Developments in Bioerosion*; Wisshak, M., Tapanila, L., Eds.; Springer: Berlin, Germany, 2008; pp. 397–413.

45. Wiersma, K.; Läbe, S.; Sander, P.M. Organic phase preservation in fossil dinosaur and other tetrapod bone from deep time. In *Fossilization: Understanding the Material Nature of Ancient Plants and Animals*; Gee, C.T., McCoy, V.E., Sander, P.M., Eds.; Johns Hopkins University Press: Baltimore, MD, USA, 2021; pp. 16–54.

46. Kibelstis, B.; Terry, D.O., Jr.; Ullmann, P. Assessment of biomechanical function as a possible control on soft tissue preservation in Eocene-Oligocene bones from the White River Group of South Dakota and Nebraska. *Geol. Soc. Am. Abstr. Programs* **2023**, *55*. [CrossRef]

47. Kibelstis, B.; Terry, D.O., Jr.; Ullmann, P. X-ray diffraction analysis of fossil bones from the Paleogene White River Group of South Dakota and Nebraska: Influence of apatite crystallinity on soft tissue preservation. *Geol. Soc. Am. Abstr. Programs* **2023**, *55*. [CrossRef]
48. Gallucci, J.E. Controls on Soft Tissue and Cellular Preservation in Late Eocene and Oligocene Vertebrate Fossils of the White River and Arikaree Groups. Master's Thesis, Temple University, Philadelphia, PA, USA, 2020; 192p.